ACS Macro Letters

Letter

pubs.acs.org/macroletters

Synthesis of Pendant Radical- and Ion-Containing Block Copolymers via Ring-Opening Metathesis Polymerization for Organic Resistive Memory

Takeo Suga,[†] Miki Sakata,[‡] Kohei Aoki,[‡] and Hiroyuki Nishide*[,‡]

[†]Waseda Institute for Advanced Study (WIAS) and [‡]Department of Applied Chemistry, Waseda University, Tokyo 169-8555, Japan

Supporting Information

ABSTRACT: Ring-opening metathesis polymerization (ROMP) using Grubbs third-generation catalyst directly yielded a norbornene-based polymer bearing robust redox-active radicals without any protection. Successive addition of imidazolium-containing norbornene in a one-pot reaction during ROMP produced pendant radical- and ion-containing block copolymers. The diode-structured thin-film devices fabricated with the obtained block polymers that had morphologies of spheres, lamellae, and inverse spheres exhibited conductive switching (write-once read-many-times, WORM) under a bias voltage, which revealed the dominant effect of the location of radicals and ions in the microphase-segregated domains on memory characteristics.

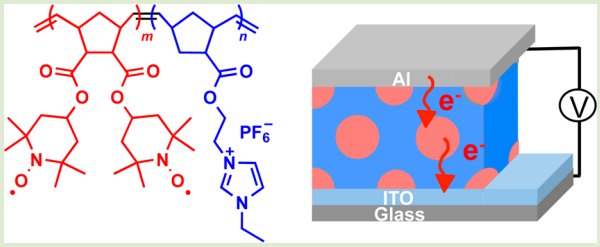

Functional polymers bearing robust but redox-active organic radicals in a pendant fashion have attracted increased attention for their superior charge-transfer and charge-storage properties.[1,2] Reversible and fast electron-exchange reactions between densely populated radical sites such as 2,2,6,6-tetramethylpiperidine-*N*-oxy (TEMPO) have enabled the utilization of these functional polymers as electrode-active materials in an organic rechargeable battery, an active layer for organic resistive memory device,[3] and as redox mediators in an organic solar cell.[4] The nitroxyl-functionalized polymer electrodes were characterized by high charge-storage capacity (110–140 mAh g^{-1}), long cycle life (exceeding 1000 cycles), and extremely high charging and discharging rate performance (full charging in a few seconds). The authors and other research groups have made a tremendous effort to design radical moieties and polymer backbones, although less attention has been paid to ion-transport associated with the redox reaction in polymer electrodes and electrode/electrolyte interface. Recently, much interest has been refocused on ionic polymers or so-called polymerized ionic liquids (PILs) as candidates for selective ion-conducting polyelectrolytes in electromechanical transducers, water purification, and biomimetic applications.[5,6] Many research groups have extensively investigated the fundamental phase behavior of PIL-based block copolymers by tuning the segment ratio and ionic association.[7−9] Beyond their scope as new electrolyte materials, here we explored the combination of two complementary components, redox-active radicals and charge-compensating ions, and developed new block copolymer-based electro-active polyelectrolytes, especially focusing on their efficient charge-transport and charge-storage properties. We also demonstrated here the modulated charge-transport even in a dry, solvent-free device, which resulted in organic resistive memory.

Our earlier work to utilize redox-active radicals and ionic salts/liquids for organic resistive memory has revealed the importance of coexistence of both components and the morphology of the matrix layer.[10] It is interesting to note that the modulated charge-transport (on/off conductive switching) was achieved by morphological variation: (a) nonswitching behavior for lamellae in parallel orientation, (b) write-once and read-many-times (WORM) memory for cylindrical morphology, and (c) rewritable and nonvolatile memory characteristics for spherical domains.[11] In our study, we designed the radical- and ion-functionalized block copolymers in a pendant fashion and correlated the memory characteristics with the location of the functional groups in selective domains.

Despite recent advances in precise polymerization techniques such as controlled radical polymerization, functional monomers bearing organic radicals still remain a challenging target owing to the termination of the propagating polymer chains by organic radicals. Our previously reported radical polymers have often been synthesized via polymerization of the corresponding precursor or protected monomers, followed by deprotection or oxidation reactions.[12] Instead, ring-opening metathesis polymerization (ROMP) using Grubbs catalysts can be a powerful tool to directly polymerize radical monomers without any protection. Based on the high catalytic activity and broad functional-group tolerance of the Grubbs catalysts, we have successfully synthesized TEMPO-functionalized poly(norbornene) via ROMP using Grubbs second-generation catalyst (G2) without any side reactions.[13] The more reactive,

Received: May 7, 2014
Accepted: July 6, 2014
Published: July 9, 2014

Scheme 1. Synthesis of Pendant Radical- and Ion-Containing Block Copolymers via ROMP

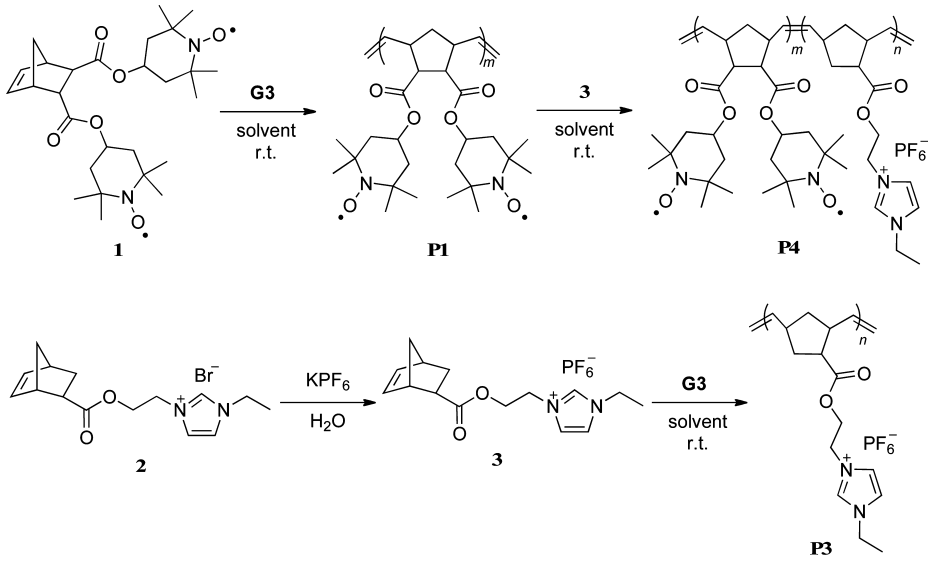

Table 1. ROMP of the Radical- and the Ion-Containing Norbornene Monomer

entry	monomer (mol·L^{-1})	G3 [M]/[C]	solvent	time	yield (%)	M_n calcd[a] (×10^3)	M_n obsd (×10^3)	PDI
1	**1** (0.1)	62.5	CH_2Cl_2	5 min	(gel)			
2	**1** (0.1)	62.5	CH_2Cl_2	1 h	6	1.8	13.4[b]	1.11
3	**1** (0.1)	62.5	CH_2Cl_2	4 h	35	11	12.9[b]	1.59
4	**1** (0.1)	62.5	CH_2Cl_2/DMF[f]	1.5 h	48	15	5.79[b]	2.18
5	**1** (0.1)	16	acetone	1 h	98	7.8	7.49[b]	1.10
6	**1** (0.1)	32	acetone	1 h	98	16	15.8[b]	1.05
7	**1** (0.1)	72	acetone	1 h	97	35	34.5[b]	1.14
8	**2** (0.2)	44	acetone	1 h				
9	**2** (0.2)	44	CH_2Cl_2/TFE[g]	24 h	75	11	11.5[c]	[e]
10	**3** (0.14)	37	CH_2Cl_2	5 min	(gel)			
11	**3** (0.14)	37	CH_2Cl_2/DMF[f]	1 h	98	15	14.7[d]	[e]
12	**3** (0.08)	37	acetone	2 h	99	15	14.8[d]	[e]

[a] M_n was calculated from the feed ratio [M]/[C] and the yield (conversion). [b] Estimated by GPC with THF as the eluent. [c] Estimated from ^{1}H NMR in DMF-d_7. [d] Estimated from ^{1}H NMR in acetone-d_6. [e] M_n and PDI were not determined by GPC due to the ionic association of the polymer. [f] CH_2Cl_2/DMF = 1/1 v/v. [g] CH_2Cl_2/TFE = 1/1 v/v.

3-bromopyridine-ligated Grubbs third-generation catalyst (G3) also yielded nitronylnitroxide-containing poly(norbornene).[14] On the other hand, norbornene derivatives bearing ionic groups have been polymerized via ROMP to the corresponding polymers of ionic liquids by other researchers.[7,15] In our study, we carefully optimized the polymerization conditions and the sequence of monomer addition to yield radical- and ion-functionalized and norbornene-based block copolymers. A thin polymer layer of separately functionalized microdomains with radical and ionic groups was employed as an active layer for the organic resistive memory, and the memory characteristics were correlated with the morphology and location of the functional groups.

The TEMPO-substituted norbornene monomer, 2,3-bis-(2′,2′,6′,6′-tetramethylpiperidinyl-*N*-oxyl-4′-oxycarbonyl)-5-norbornene, **1**, was prepared via the esterification of 5-norbonene-2,3-dicarboxylic anhydride using the Mukaiyama reagent according to our previous paper.[11] The ionic norbornene monomer, *exo*,*endo*-5-norbornene-2-yl carboxyethyl-3-ethylimidazolium bromide, **2**, was synthesized in three steps from *exo*,*endo*-5-norbornene-2-yl carboxylic acid by reference.[7] After an anion-exchange reaction, *exo*,*endo*-5-norbornene-2-yl carboxyethyl-3-ethylimidazolium hexafluorophosphate, **3**, was obtained. The synthetic details are shown in Supporting Information.

The ring-opening metathesis polymerization of the radical- or ion-containing norbornene monomer was examined prior to block copolymerization (Scheme 1). Table 1 summarizes the polymerization results of TEMPO-substituted norbornene **1** via ROMP using Grubbs third-generation catalyst (**G3**) in various organic solvents. In dichloromethane, the viscosity of the polymerization solution increased significantly after 5 min to yield a partially insoluble gel (entry 1). Further stirring of the polymerization mixture produced a homogeneous state in the end; however, the polymer yield, molecular weight (M_n), and polydispersity index (PDI) were not controlled (entries 2 and 3). The polymerization of **1** in the mixed solvents (CH_2Cl_2/DMF = 1/1 v/v) also produced a high-molecular-weight polymer, but a relatively wide PDI (2.2) was obtained among the polymers prepared by ROMP (entry 4). By using acetone as the polymerization solvent instead, the polymerization of **1** proceeded quantitatively at a moderate polymerization rate (1 h), and the molecular weights were tunable with the monomer/catalyst [M]/[C] feed ratio (entries 5−7). The electron-spin resonance (ESR) spectrum showed a strong unimodal peak at g = 2.0064, which is ascribed to the densely populated NO

dx.doi.org/10.1021/mz500273z | *ACS Macro Lett.* 2014, 3, 703−707

radicals along a polymer chain. The obtained polymer **P1** was slightly orange in color, which is attributed to the nitroxide radical. The radical density of **P1** was estimated from both integration of the ESR signal and Curie plots and the saturated magnetization, using the superconducting quantum interference device (SQUID); the value was 1.94 radicals per monomer unit, for example, for entry 5's **P1**, which strongly supports the durability of TEMPO against **G3** during polymerization. The obtained radical polymer, **P1**, was soluble in tetrahydrofuran, chloroform, toluene, acetone, and DMF, and was slightly soluble in acetonitrile.

ROMP of the ionic monomer **2** was carried out using **G3** in acetone, but the insoluble polymer precipitated during the polymerization because of the low solubility of imidazolium bromide salt (entry 8). A dichloromethane/2,2,2-trifluoroethanol (1/1 v/v) mixed solvent was used instead, but the polymerization rate was very slow (10% conversion after 1 h and 75% conversion after 24 h, entry 9). Considering the solvent compatibility, the anion-exchange reaction to hexafluorophosphate was employed. Polymerization of the ionic monomer **3** was examined using **G3** in various solvents. Although the polymerization in CH_2Cl_2 yielded an insoluble gel (entry 10), polymerization in the mixed solvents (CH_2Cl_2/DMF) or acetone proceeded well to form high-molecular-weight polymers (entries 11 and 12). The obtained ionic polymer, **P3**, was soluble in acetone and DMF, but insoluble in toluene.

Based on the polymerization results of **1** and **3**, acetone was selected as a cosolvent to accomplish successive block copolymerization of **1** and **3** in a one-pot reaction. For the sequence of monomer addition, the TEMPO-substituted norbornene, **1**, was chosen as the first monomer because the chain extension of a neutral monomer from an ionic macromer often forms a micelle during polymerization. Otherwise, the change in solubility of the propagating ionic block copolymers during the polymerization should be considered carefully. It was also beneficial to quickly monitor the molecular weight of the first block by gel permeation chromatography (GPC; ionic polymers often form ionic aggregates, and it is not trivial to measure the molecular weight properly). To ensure the consumption of all monomer **1**, the polymerization was carried out for 1 h before addition of the second monomer **3**. Results of the controlled ROMP for the block copolymerization are summarized in Table 2.

Table 2. Block Copolymerization of 1 and 3[a]

entry	composition[b] m/n	M_n (first block)[c] ($\times 10^3$)	M_n (total)[d] ($\times 10^3$)	yield (%)
1	0.09:0.91	6.4	61	94
2	0.42:0.58	15	31	97
3	0.84:0.16	32	37	95

[a]0.1 M in acetone, polymerization time = 1 h each. [b]Estimated by ^{1}H NMR. [c]Estimated by GPC with THF as eluent. [d]M_n was calculated from M_n of first block and composition.

Quenching of the TEMPO radical moiety in the polymers with phenylhydrazine enabled NMR studies to characterize the obtained polymers. It should be noted that deuterated solvents were carefully selected because the use of selective solvents such as dimethyl sulfoxide (DMSO-d_6) for ionic segments often induced micelle formation, and the ^{1}H peaks for the core domain were underestimated (see Supporting Information for details). We selected DMF-d_7 for ^{1}H NMR spectroscopy. In the diffusion-ordered spectroscopy (DOSY) spectrum of polymer **P4**, all peaks corresponding to both **P1** and **P3** segments were recorded with the same diffusion constant (D in Figure 1).

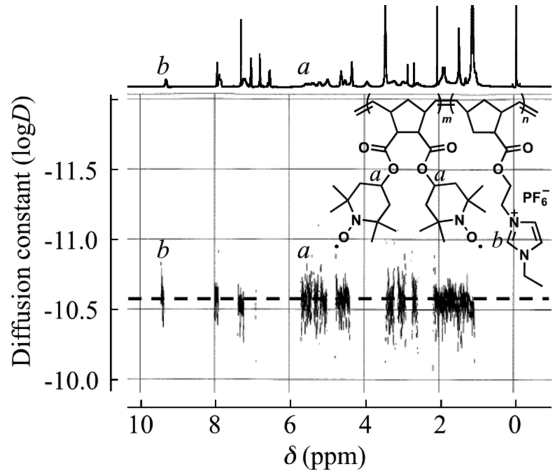

Figure 1. DOSY spectrum of the block copolymer **P4** (entry 2) in DMF-d_7.

These results indicate that the second monomer, **3**, was polymerized from the chain end of **P1** and any homopolymer **P1** was absent in the product. A ^{1}H NMR spectrum of the obtained polymer (in DMF-d_7) showed peaks ascribed to both the piperidine C*H* (peak *a*) on the **P1** segment (δ = 5.62) and the imidazolium NC*H*N (peak *b*) on the **P3** segment (δ = 9.20). The radical segments of the obtained copolymers estimated with the NMR peak integrations were in the range of 9 to 84 mol %, which agree well with those estimated from the SQUID measurement. We thus conclude that the radical and ion segment ratios in the block copolymers were in tune with the monomer feed ratio.

The morphologies of the obtained radical- and ion-containing block copolymers were investigated with atomic force (scanning probe) microscopy (AFM) on the thin layer (~150 nm) of polymer **P4**. An acetonitrile solution of each polymer was spin-coated on a silicon substrate and annealed under various organic solvent vapors such as acetonitrile, THF, and toluene (see Supporting Information). THF was chosen as the selective solvent for the ionic segment, and toluene was chosen as the selective solvent for the radical (neutral) segment. The AFM phase images clearly exhibited a microphase separation with a length scale of 20 nm, albeit without long-range order. Based on the composition of the obtained block copolymers and the preliminary indications of AFM indicated that the morphologies are likely to be sphere, lamella, inverse sphere (Figure 2a–c). These results indicate that we attained functional nanostructures with tailored morphology based on the radical- and ionic-segment ratios, and at the same time, each domain was functionalized separately.

We reported in our previous paper that the coexistence of redox-active radicals and charge-compensating ions in the monolayered device is required for the active layer of the resistive memory (see more detail in Supporting Information, Figure S3);[10,11] however, the location of each embedded functionality had not been examined. In the study reported here, we utilized the block copolymer **P4** film as an active layer with separate radical- and ion-domains to elucidate the effect of

dx.doi.org/10.1021/mz500273z | ACS Macro Lett. 2014, 3, 703–707

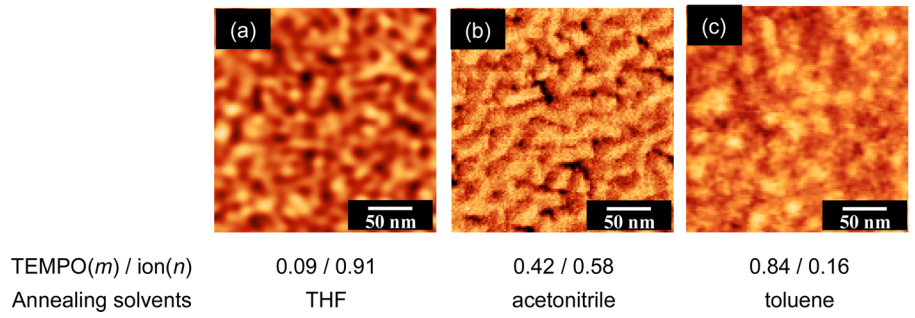

Figure 2. AFM phase images of polymer **P4** (entries 1–3) after solvent annealing.

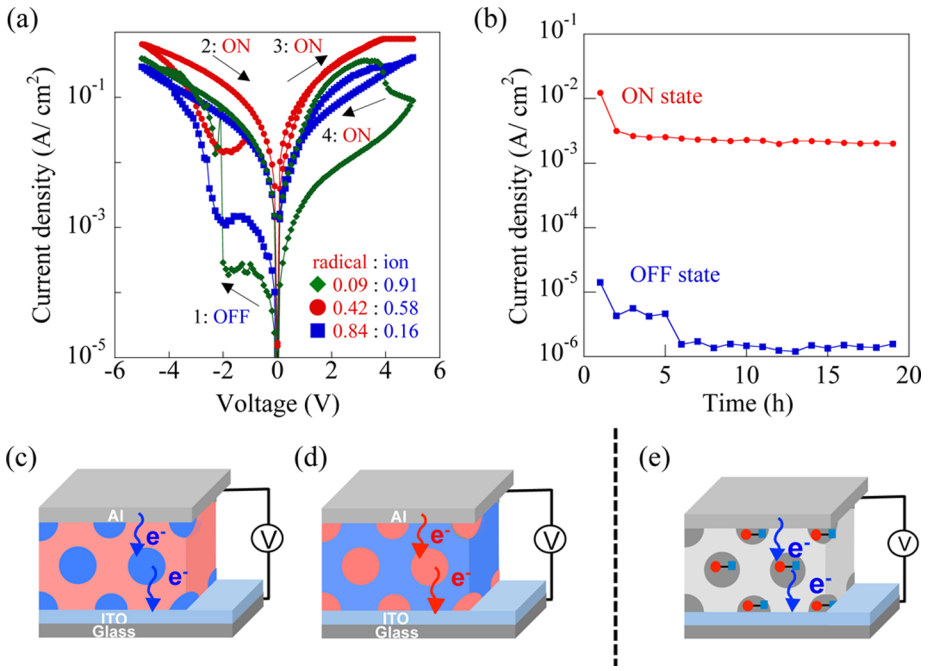

Figure 3. (a) *I*–*V* characteristics of devices with the layered configuration of ITO/block copolymer **P4**/Al. The mole fractions of radicals in block copolymer **P4** were 9 (▲), 42 (●), and 84 mol % (■). (b) Retention time of the devices. (c–e) Device configurations.

functional group location on memory characteristics in addition to the morphological variation.

Diode-structured thin-film devices were fabricated with the block copolymer **P4**. The block copolymer layers (100 nm in thickness) were prepared by spin-coating the THF solutions of **P4** with different segment ratios and then subjecting them to annealing under the solvent vapor. The top aluminum electrode was deposited by thermal evaporation under vacuum to form the diode-structured or monolayered devices. Typical *I*–*V* characteristics of the fabricated devices are shown in Figure 3a. Upon application of a bias voltage in the negative direction (0 to −5 V), the current density for all devices drastically increased at around −3 V as the threshold voltage and had an ON/OFF current ratio of ∼10^3. The devices did not show any switch back to the high resistive (OFF) state upon application of the positive bias scan (0 to 5 V). The durability of both ON and OFF states was verified by experiments to measure the retention time (Figure 3b). In our previous study, we discovered morphology-driven charge-transport and proposed that a device with spherical morphology containing both radical and ionic components would serve as rewritable memory (Figure 3e). However, even with spherical domains, the devices fabricated with polymer **P4** exhibited only WORM memory characteristics, which revealed new insights that radicals and ions localized in the separate domains critically affected the memory characteristics rather than the morphology.

In summary, we synthesized radical- and ion-functionalized block copolymers via Grubbs-catalyzed ring-opening metathesis polymerization. The combination of redox-active radicals and charge-compensating ions enabled the utilization of the copolymer as an active layer for organic resistive memory, and the resulting device exhibited WORM-type memory characteristics in both spherical and lamellae morphologies. Besides morphological modulation of charge-transport, this work revealed, for the first time, that the location of the functional groups is also a critical factor for tuning memory characteristics. To further understand the mechanism, our group is conducting an ongoing study using in situ scanning probe microscopy under an applied bias, such as that in conductive atomic force microscopy.

■ ASSOCIATED CONTENT

Supporting Information

Experimental details. This material is available free of charge via the Internet at http://pubs.acs.org.

dx.doi.org/10.1021/mz500273z | *ACS Macro Lett.* 2014, 3, 703–707

AUTHOR INFORMATION

Corresponding Author

*E-mail: nishide@waseda.jp.

Notes

The authors declare no competing financial interest.

ACKNOWLEDGMENTS

This work was partially supported by Grants-in Aid for Scientific Research (Nos. 24225003 and 23550139) from MEXT, Japan. T.S. acknowledges the MEXT/JST tenure-track program and the MIZUHO Foundation.

REFERENCES

(1) (a) Nishide, H.; Oyaizu, K. *Science* **2008**, *319*, 737−738. (b) Nishide, H.; Iwasa, S.; Pu, Y.-J.; Suga, T.; Nakahara, K.; Satoh, M. *Electrochim. Acta* **2004**, *50*, 827. (c) Nakahara, K.; Oyaizu, K.; Nishide, H. *Chem. Lett.* **2011**, *40*, 222. (d) Suga, T.; Ohshiro, H.; Sugita, S.; Oyaizu, K.; Nishide, H. *Adv. Mater.* **2009**, *21*, 1627−1630. (e) Suga, T.; Sugita, S.; Ohshiro, H.; Oyaizu, K.; Nishide, H. *Adv. Mater.* **2011**, *23*, 751−754.

(2) For reviews and book chapters: (a) Nishide, H.; Suga, T. *Electrochem. Soc. Interface* **2005**, *14* (4), 32. (b) Suga, T.; Nishide, H. In *Stable Radicals - Fundamentals and Applied Aspects of Odd-Electron Compounds*; Hicks, R. G., Ed.; Wiley-VCH: Weinheim, 2010, Ch. 14, pp 507−519. (c) Oyaizu, K.; Nishide, H. Polyradicals in Batteries. *Encyclopedia of Radicals in Chemistry, Biology and Materials*; Wiley: New York, 2012. (d) Poizot, P.; Dolhem, F. *Energy Environ. Sci.* **2011**, *4*, 2003. (e) Janoschka, T.; Hager, M. D.; Schubert, U. S. *Adv. Mater.* **2012**, *24*, 6397.

(3) (a) Yonekuta, Y.; Susuki, K.; Oyaizu, K.; Honda, K.; Nishide, H. *J. Am. Chem. Soc.* **2007**, *129*, 14128. (b) Lee, J.; Lee, E.; Kim, S.; Bang, G.-S.; Shultz, D. A.; Schmidt, R. D.; Forbes, M. D. E.; Lee, H. *Angew. Chem., Int. Ed.* **2011**, *50*, 4414−4418.

(4) Kato, F.; Kikuchi, A.; Okuyama, T.; Oyaizu, K.; Nishide, H. *Angew. Chem., Int. Ed.* **2012**, *51*, 10177−10180.

(5) (a) *Electrochemical Aspects of Ionic Liquids*; Ohno, H., Ed.; Wiley-Interscience: New York, 2005. (b) Ohno, H.; Ito, K. *Chem. Lett.* **1998**, 751. (c) Yoshio, M.; Kagata, T.; Hoshino, K.; Mukai, T.; Kato, T. *J. Am. Chem. Soc.* **2006**, *128*, 5570.

(6) (a) Green, M. D.; Long, T. E. *Polym. Rev.* **2009**, *49*, 339. (b) Yuan, J.; Mecerreyes, D.; Antonietti, M. *Prog. Polym. Sci.* **2013**, *38*, 1009. (c) Hickner, M. A.; Herring, A. M.; Coughlin, E. B. *J. Polym. Sci., Part B.: Polym. Phys.* **2013**, *51*, 1727.

(7) (a) Vygodskii, Y. S.; Shaplov, A. S.; Lozinskaya, E. I.; Filippov, O. A.; Shubina, E. S.; Bandari, R.; Buchmeiser, M. R. *Macromolecules* **2006**, *39*, 7821−30. (b) Wiesenauer, E. F.; Edwards, J. P.; Scalfani, V. F.; Bailey, T. S.; Gin, D. L. *Macromolecules* **2011**, *44*, 5075−8. (b) Scalfani, V. F.; Wiesenauer, E. F.; Ekblad, J. R.; Edwards, J. P.; Gin, D. L.; Bailey, T. S. *Macromolecules* **2012**, *45*, 4262−4276.

(8) (a) Lodge, T. P. *Science* **2008**, *321*, 50. (c) Zhang, S.; Lee, K. H.; Frisbie, C. D.; Lodge, T. P. *Macromolecules* **2011**, *44*, 940. (d) Cho, J. H.; Lee, J.; He, Y.; Kim, B.-S.; Lodge, T. P.; Frisbie, C. D. *Adv. Mater.* **2008**, *20*, 686.

(9) (a) Green, M. D.; Choi, J.-H.; Winey, K. I.; Long, T. E. *Macromolecules* **2012**, *45*, 4749. (b) Gwee, L.; Choi, J.-H.; Winey, K. I.; Elabd, Y. A. *Polymer* **2010**, *51*, 5516. (c) Choi, U. H.; Lee, M.; Wang, S.; Liu, W.; Winey, K. I.; Gibson, H. W.; Colby, R. H. *Macromolecules* **2012**, *45*, 3974.

(10) Suga, T.; Takeuchi, S.; Ozaki, T.; Sakata, M.; Nishide, H. *Chem. Lett.* **2009**, *38*, 1160.

(11) Suga, T.; Takeuchi, S.; Nishide, H. *Adv. Mater.* **2011**, *23*, 5545.

(12) (a) Suga, T.; Pu, Y.-J.; Kasatori, S.; Nishide, H. *Macromolecules* **2007**, *40*, 3167. (b) Sukegawa, T.; Omata, H.; Masuko, I.; Oyaizu, K.; Nishide, H. *ACS Macro Lett.* **2014**, *3*, 240.

(13) Suga, T.; Konishi, H.; Nishide, H. *Chem. Commun.* **2007**, 1730.

(14) Sukegawa, T.; Kai, A.; Oyaizu, K.; Nishide, H. *Macromolecules* **2013**, *46*, 1361−1367.

(15) Vygodskii, Y. S.; Shaplov, A. S.; Lozinskaya, E. I.; Lyssenko, K. A.; Golovanov, D. G.; Malyshkina, I. A.; Gavrilova, N. D.; Buchmeiser, M. R. *Macromol. Chem. Phys.* **2008**, *209*, 40−51.